Erzincan Üniversitesi
Fen Bilimleri Enstitüsü Dergisi
2024, 17(3), 797-810
ISSN: 1307-9085, e-ISSN: 2149-4584
Araştırma Makalesi

Erzincan University
Journal of Science and Technology
2024, 17(3), 797-810
DOI: 10.18185/erzifbed.1510542
Research Article

Voltage Controlled Oscillator Realisation with Temperature and Source Independent Circuits

Müslüm GÜR*[1], Yunus BABACAN[2]

[1]Çankırı Karatekin University, Vocational School, Department of Electronics and Automation, 18100, Çankırı, Turkey

[2]Erzincan Binali Yıldırım University, Faculty of Engineering and Architecture, Department of Electrical and Electronics Engineering, 24100, Erzincan, Turkey

Received: 04/07/2024, **Revised:** 28/08/2024, **Accepted:** 18/09/2024, **Published:** 31/12/2024

Abstract

In this article, a square wave was generated with a voltage-controlled oscillator circuit (VCO) using a bandgap reference voltage circuit and a low drop-out (LDO) circuit. The band gap reference circuit can generate a constant 500mV voltage between -40ºC and +125ºC. The LDO circuit is driven by a bandgap reference voltage circuit and exhibits a stable output even at different voltage levels. The last circuit, VCO, is driven by the LDO circuit. It can generate square waves between 1200MHz and 1600MHz at the output. Simulations using 130nm TSMC technology parameters have been successfully achieved.

Keywords: Bandgap reference voltage circuit, low dropout regulator circuit, voltage controlled oscillator circuit.

Sıcaklıktan ve Kaynaktan Bağımsız Devreler ile Voltaj Kontrollü Osilatör Gerçeklenmesi

Öz

Bu makalede, band aralığı referans gerilim devresi ve düşük düşümlü regülatör devresi (LDO) kullanılarak gerilim kontrollü salınıcı devresi (VCO) ile kare dalga üretildi. Band aralığı referans devresi -40ºC ile +125ºC arasında sabit 500mV gerilim üretebilmektedir. LDO devresi ise band aralığı referans gerilim devresi ile sürülmekte olup farklı gerilim seviyelerinde bile kararlı bir çıkış sergilemektedir. Son devre olan VCO ise LDO devresi tarafından sürülmektedir. Çıkışta 1200MHz ile 1600MHz arasında kare dalga üretebilmektedir. 130nm TSMC teknoloji parametreleri kullanılarak yapılan benzetimler başarılı bir şekilde elde edilmiştir.

Anahtar Kelimeler: Bant aralığı referans gerilim devresi, düşük çıkışlı regülatör devresi, gerilim kontrollü osilatör devresi.

*Corresponding Author: muslumgur@karatekin.edu.tr
Müslüm GÜR, https://orcid.org/0000-0002-4842-5345
Yunus BABACAN, https://orcid.org/0000-0002-6745-0626

1. Introduction

In order to obtain circuits to operate with good performance, voltage reference circuits that are independent of temperature and power supply fluctuations are required [1],[2]. It is possible to find many reference voltage circuits with different features in the literature [3-6]. Especially, it is important to design sub-1v supply circuits [7].

Low drop-out (LDO) circuits are used as power supplies in RF, analog and mixed signal applications [8]. In noise-sensitive systems, a low-output regulator is generally used after the DC-DC converter stage to meet the power need. In LDO circuits, wide loop bandwidth and fast response time are important at the design stage, and studies that take these parameters into consideration can be easily found in the literatüre[9-10].

Voltage controlled oscillators (VCO) are circuits that are widely used in many applications and can produce square waves even at high frequencies. Ring oscillators and LC oscillators can also be used as voltage-controlled oscillators. Ring oscillators are types of oscillators obtained by connecting the last delay stage to the first delay stage [11]. If the delay multiples increase, the frequency of the produced signal decreases and its cost increases[12-13].

In this study, the band gap reference voltage circuit, LDO circuit and VCO circuit found in the literature were rearranged for the desired purposes and turned into a block that can work together. Bandgap reference circuit exhibited high performance from -40ºC to 125ºC. LDO circuit also exhibited similar performance under connected capacitor and current source as load. The last circuit, VCO, generated a close to ideal square wave at the desired frequencies even under load. For all simulations, TSMC 130nm parameters were are used to analyze the circuits and all results are obtained with high performance.

2. Material and Methods

2.1.Bandgap Reference Voltage Circuit

While designing the bandgap reference voltage circuit, the opposite temperature coefficients of PMOS and NMOS transistors were used. There are many transistor models, and in this study, mathematical analyzes were made using the α power model [14]. V_{GS} voltage,

$$V_{GS\_ZTC} = V_{TH0} - \eta T + \frac{\alpha \eta T_0}{\beta}\left(\frac{T}{T_0}\right)^{\frac{\beta}{\alpha}} \tag{2.1}$$

When the first order derivative of the above expression is taken with respect to temperature,

$$\frac{dV_{GS\_ZTC}}{dT} = -\eta + \eta\left(\frac{T}{T_0}\right)^{(\frac{\beta}{\alpha}-1)} \tag{2.2}$$

Similarly, when the above expression is derived one more degree with respect to temperature,

$$\frac{d^2V_{GS\_ZTC}}{dT^2}=\left(\frac{\beta}{\alpha}-1\right)\eta T_0^{(\frac{\beta}{\alpha}-1)}T^{(\frac{\beta}{\alpha}-2)} \tag{2.3}$$

Here, V_{THO} is the threshold voltage at zero Kelvin, η, α, β are constant coefficients, and when the second order derivative is equal to zero, the β value must be equal to the α value. This ensures that transistors operate independently of temperature. Although the β value is fixed and 1.5, the α value varies between 1 and 2. For a value equal to 1, the transistor must be operated in the active region, and for a value greater than 1, it must be operated in the saturation region. Since both values (α, β) must be equal, the two values become equal thanks to the saturation operation of the transistors.

As seen in Figure 1, the tail current of the OTA (Operational Transconductance Amplifier) circuit is created by the M_{A9} transistor driven by the voltage created with the help of the M_{A1}-M_{A4} transistors. A simple OTA structure was used, consisting of OTA M_{A5}-M_{A9} transistors, and its output was connected to the gate terminals of M_{A10}-M_{A11} transistors to drive them. In addition, the required current for the LDO circuit was created with the help of M_{A14}-M_{A16} transistors.

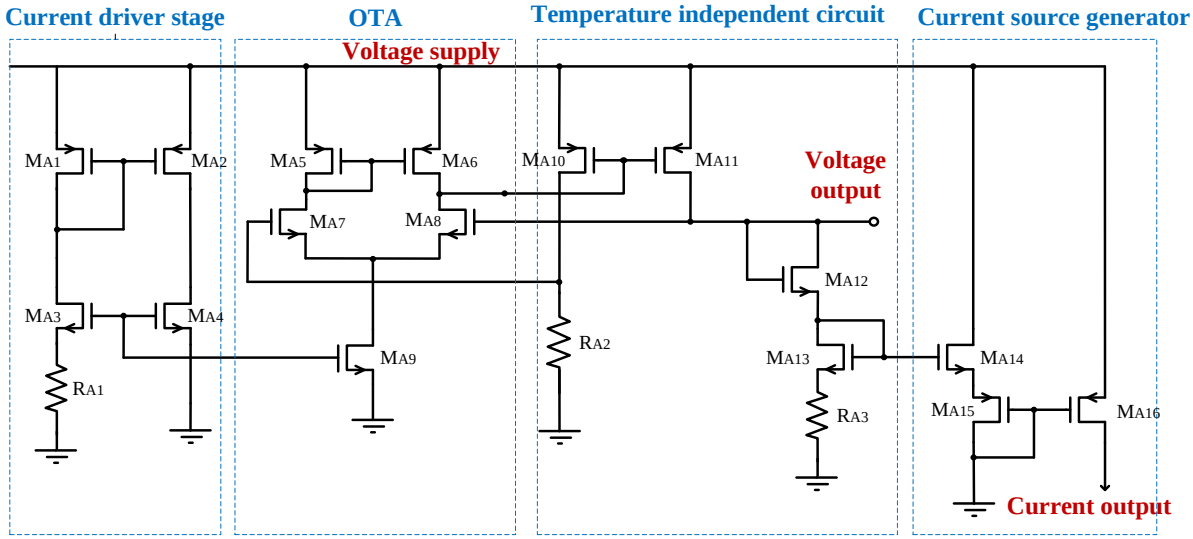

Figure 1. Modified temperature independent bandgap reference circuit[14]

The dimensions of the transistors in the circuit and the values of the elements used are important to obtain the 500mV voltage value. Table 1 contains information about circuit elements.

Table1. Element dimensions and values of the circuit.

Circuit Element	W(µm)	L(µm)	Circuit Element	W(µm)	L(µm)
$M_{A1\text{-}A2}$	2	1	M_{A12}	16.1	1.3
$M_{A3\text{-}A4}$	4	4	M_{A13}	8.1	1
$M_{A5\text{-}A6}$	16	4	M_{A14}	10	1

M_{A7-A8}	16	2	$M_{A15-A16}$	1	1
M_{A9}	3	1	R_{A1}	10 kΩ	
M_{A10}	16	2	R_{A2}	110 kΩ	
M_{A11}	16.2	2	R_{A3}	120 Ω	

As seen in Figure 2a, a temperature-independent voltage value of 500mV was successfully obtained. The temperature changed from -40ºC to 125ºC with 5ºC temperature steps.

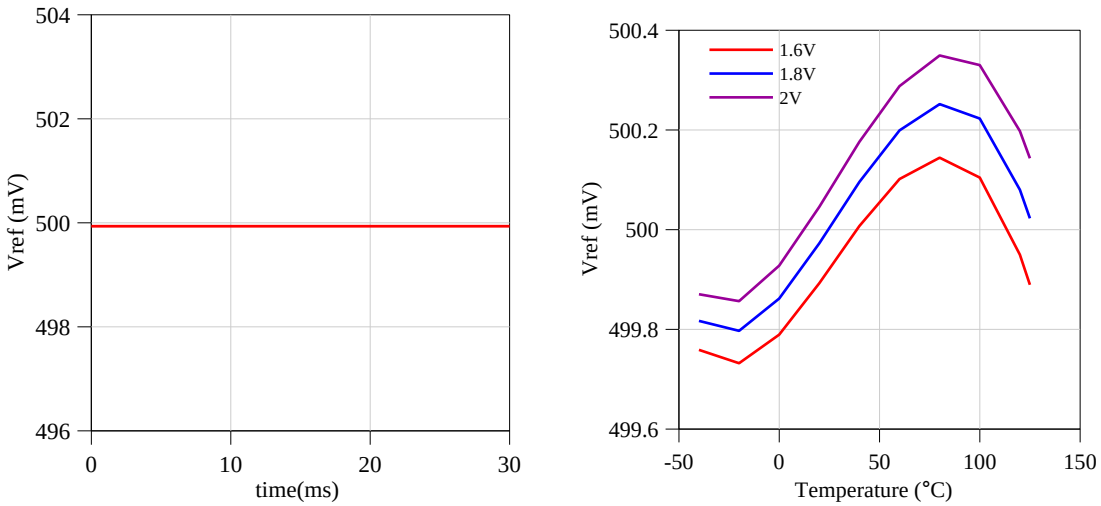

(a) **(b)**

Figure 2. a) Time-dependent reference voltage output **b)** the reference voltage output for different supply voltages.

The output voltage of the circuit according to different supplies is seen in Figure 2b. As can be seen from the figure, the circuit exhibits a very stable output despite the wide temperature range, showing a change of 5.5 ppm/°C. Finally, the frequency-dependent variation of the power supply rejection ratio (PSRR) value was obtained in Figure 3 and was found to be -20dB on average.

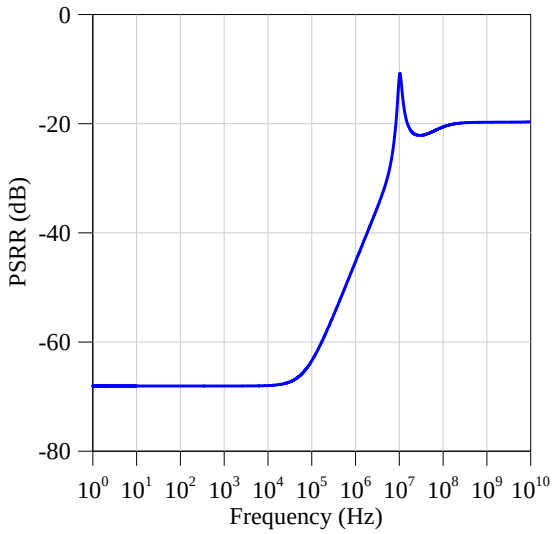

Figure 3. The change of PSRR value depending on frequency.

2.2. LDO Voltage Regulator Circuit

Low output regulator (LDO) circuits are used extensively in many analog circuits due to their features such as low power consumption, high power supply rejection ratio (PSRR) and high current capability [8]. Many different types of LDO circuits can be found in the literature [15-18]. The LDO circuit [19] found in the literature, which will be used for the square wave generator, has been modified. The block diagram of the circuit is shown in the figure 4. Here, while reference voltage is applied from the positive input of the opamp, feedback is provided from the other input. A high current block was added to the circuit to provide the high current (a few mA) required for the oscillator circuit.

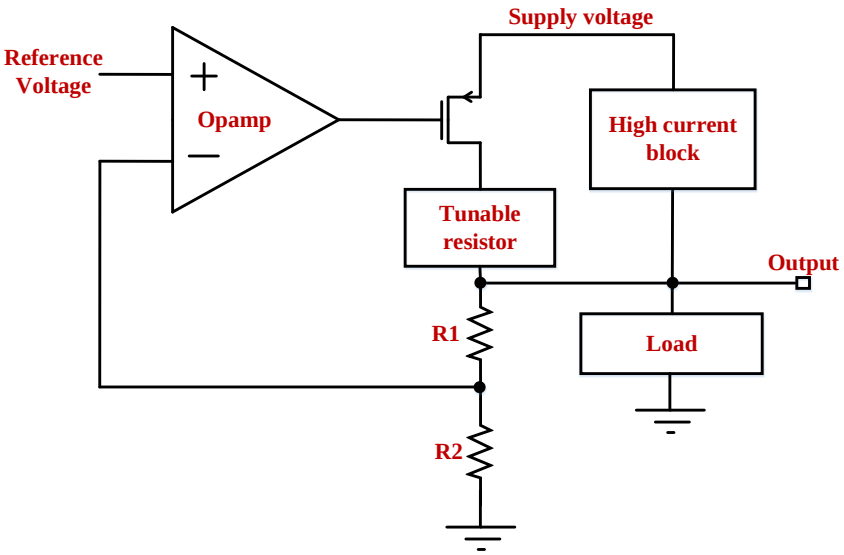

Figure 4. Block diagram of the LDO circuit.

As seen in the circuit in figure 5, the LDO circuit consists of three blocks. These are the opamp section where amplification and comparison are performed, the variable and fixed resistance region for feedback and voltage level control, and the high current block to provide high current.

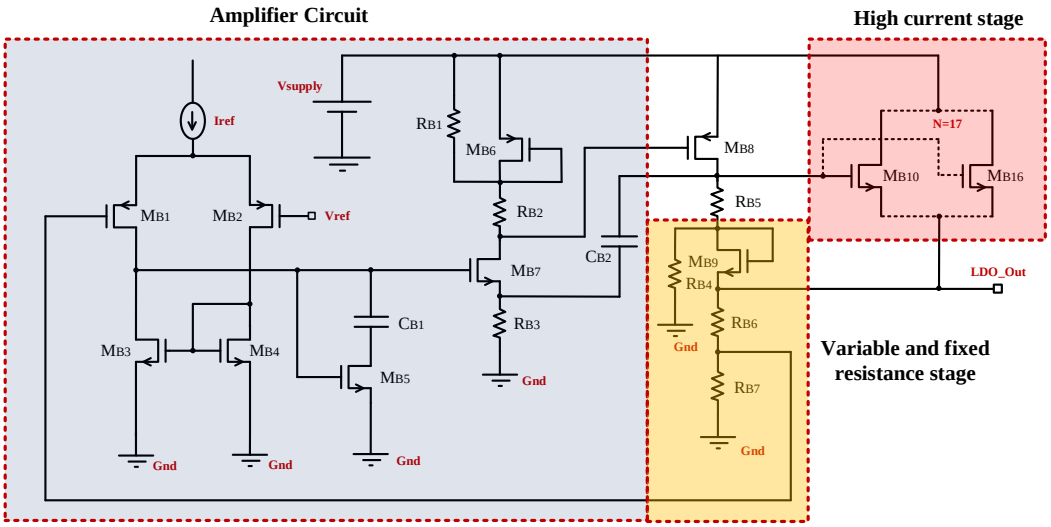

Figure 5. Modified LDO circuit diagram [19].

Here, capacitor C_{B1} provides impedance matching thanks to its high resistance at low frequencies and low resistance at high frequencies. C_{B2} capacitor is also used to improve the power supply rejection ratio (PSRR) value. M_{B6}-M_{B9} transistors are transistors used to adjust the current given to the load at the output. The current drawn by the load occurs through the M_{B8} and M_{B9} transistors and the R_{B5} resistor. Here, resistors R_{B2} and R_{B5} are used to limit unnecessary current flow and therefore excessive power consumption. Resistors R_{B1} and R_{B4} are also used to regulate current flow when there is no load. M_{B8} transistors, generally called power transistors, are implemented with PMOS transistors. However, in this design, NMOS transistor was used due to its higher electron mobility and lower parasitic capacitances compared to PMOS transistor. The dimensions and element values of the elements of the circuit are given in table 2. Here, care has been taken to create a circuit suitable for chip implementation, especially by choosing low capacitor values.

Table 2. Element dimensions and values of the circuit.

Circuit Element	W(µm)	L(µm)	Circuit Element	Element values
$M_{B1-2,6}$	2	1	C_{B1}	3pF
$M_{B3-5,7,9}$	1	1	C_{B2}	10pF
M_{B10-16}	30	0.25	R_{B1}	100kΩ
R_{B2}	30kΩ		R_{B3}	1kΩ
R_{B4}	10kΩ		R_{B6}	146kΩ
R_{B5}	200kΩ		R_{B7}	110kΩ

When the input is 1.8V, the output voltage is measured as 1.2V. As seen in Figure 6a, the output was measured as a stable and constant value when 500pF load capacitor is connected. Likewise, when the input voltage was set to 2.5V, the time-dependent change of the output voltage was measured. It can be easily seen in Figure 6b, even if the input voltage changes radically, the output voltage changes very little.

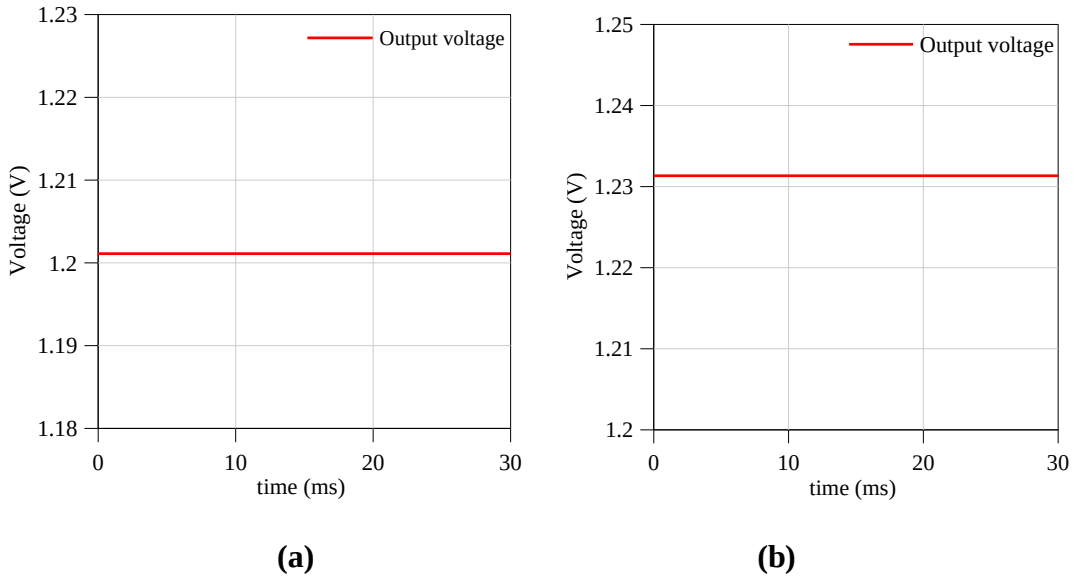

(a) **(b)**

Figure 6. a) The variation of output voltage with time when the input voltage is 1.8V and **b)** 2.5V.

When the loop gain and phase margin of the LDO circuit are analyzed, it appears as shown in Figure 7. It is desired that the gain and phase angle of the LDO circuit be high. As seen in Figure 2.8, 108.06dB and 117.07º were obtained.

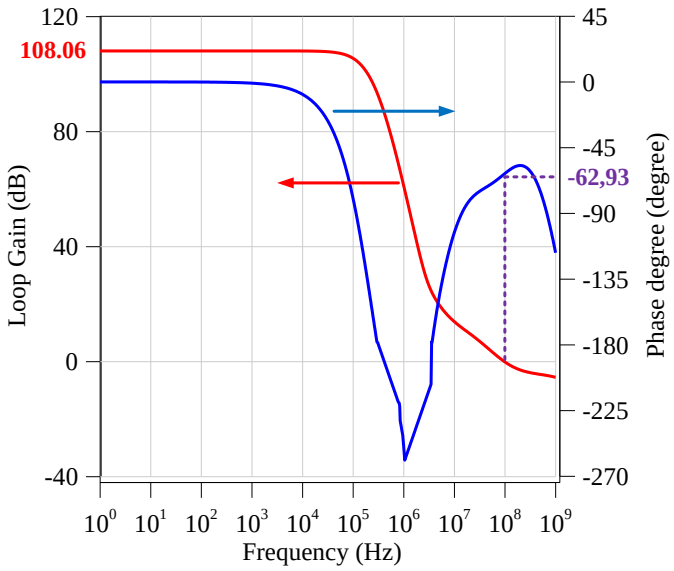

Figure 7. Loop gain and phase margin changes.

2.3. Voltage Controlled Oscillator (VCO) Circuit

Voltage controlled oscillator (VCO) circuits are advantageous circuit types due to their low power consumption and suitability for VLSI circuits. There are different types of VCO circuits in the literature [20-22]. In this study, the modified circuit is seen in Figure 8 and consists of two basic blocks. The first block is the part where the square wave signal is produced, and the second block is the block required to provide enough current when the load is connected. The first block consists of 3 parts. The first part; It consists of the current supply stage, the inverter stage where the signal is generated, and the current limiting stage that provides current limitation. As the number of inverter stages increases, the generated signal decreases inversely. To operate at high frequencies, inverter stages must be increased.

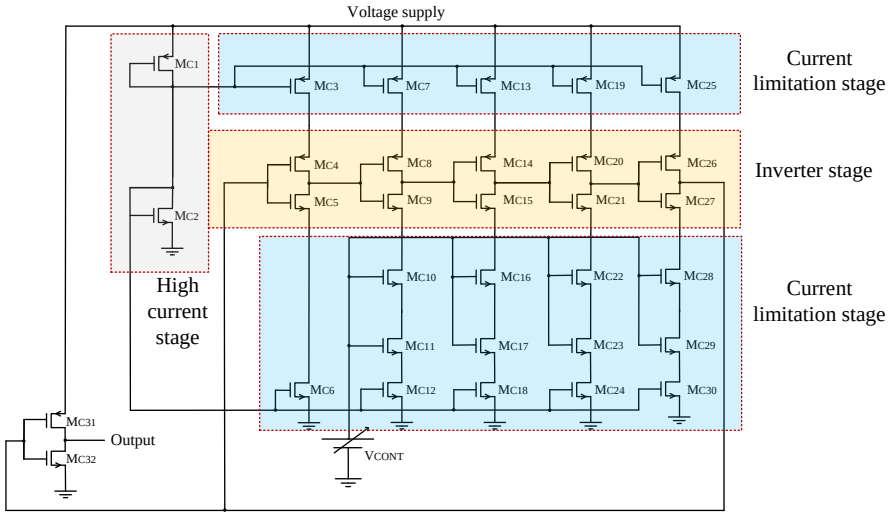

Figure 8. Modified VCO circuit [20]

In addition, M_{C11}, M_{C17}, M_{C23} and M_{C29} transistors enable the K_{VCO} value to be improved. These transistors take an active role in reducing the effect of changing the V_{CONT} value. Transistor dimensions and element values of the designed circuit are given in table 3.

Table 3. The element dimensions and values for the circuit.

Circuit Element	W(µm)	L(µm)	Circuit Element	W(µm)	L(µm)
M_{C1}	2	1	$M_{C16,17,22,23}$	0.7	0.2
M_{C2}	1	2	M_{28}	2	0.2
M_{C3}	25	0.5	M_{C29}	1	0.2
$M_{C4\text{-}5,8\text{-}9,14,15,20,21,26,27}$	0.3	0.2	$M_{C31\text{-}32}$	1	0.3
$M_{C10\text{-}11}$	0.5	0.2	$M_{C33\text{-}34}$	3	0.3
$M_{C6,12,18,24,30}$	14	0.35	$M_{C35\text{-}36}$	10	0.3
$M_{C7,13,19,25}$	15	0.5	$M_{C39\text{-}64}$	30	0.3

The VCO circuit is supplied with 1.2V supplied from the LDO circuit. It has been successfully achieved that the designed circuit produces a square wave between 0V-1.1V and its frequency is controlled with a voltage source. Here, the control voltage value was set to 0.6V to generate the signal and the signal at 1.2GHz was produced as seen in figure 9. Likewise, when the control voltage was set to 1.1V, the output voltage was easily obtained as 1.6GHz without distorting the signal shape.

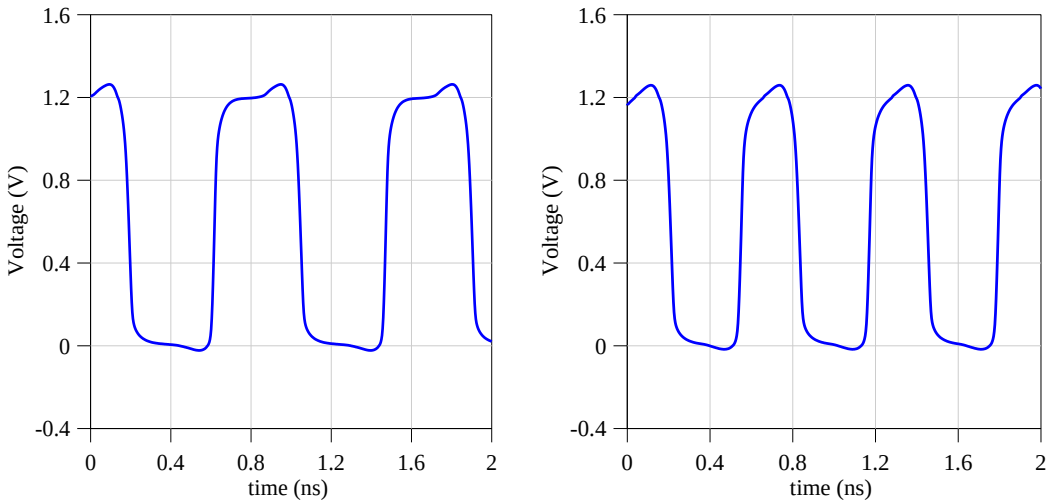

(a) **(b)**

Figure 9. Signal generated by the VCO circuit **a)** 1.2GHz **b)** 1.6GHz.

K_{VCO} value is a quantity that indicates the relationship between the control voltage and the produced frequency. It is desirable that the generated frequency is not too sensitive to the control voltage. Figure 10 shows the change in the frequency generated by the control voltage.

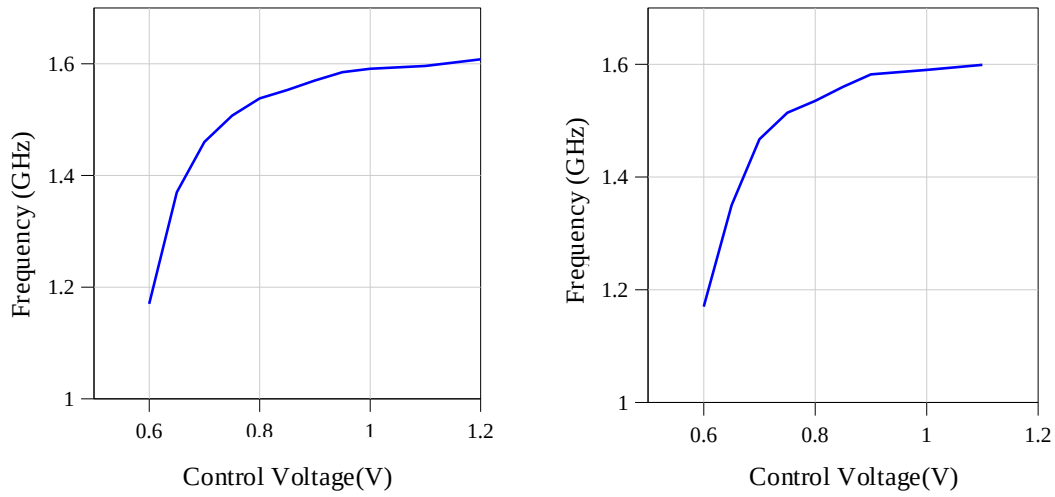

(a) **(b)**

Figure 10. Variation of frequency with control voltage **a)** with no load **b)** with 0.6pF load. Here, the K_{VCO} value is 730 MHz/V.

Another important advantage of the modified VCO circuit is the duty cycle value of the produced square wave. Here, if these ratios for 1200MHz and 1600MHz frequencies are calculated as in figure 11, the results are obtained as follows.

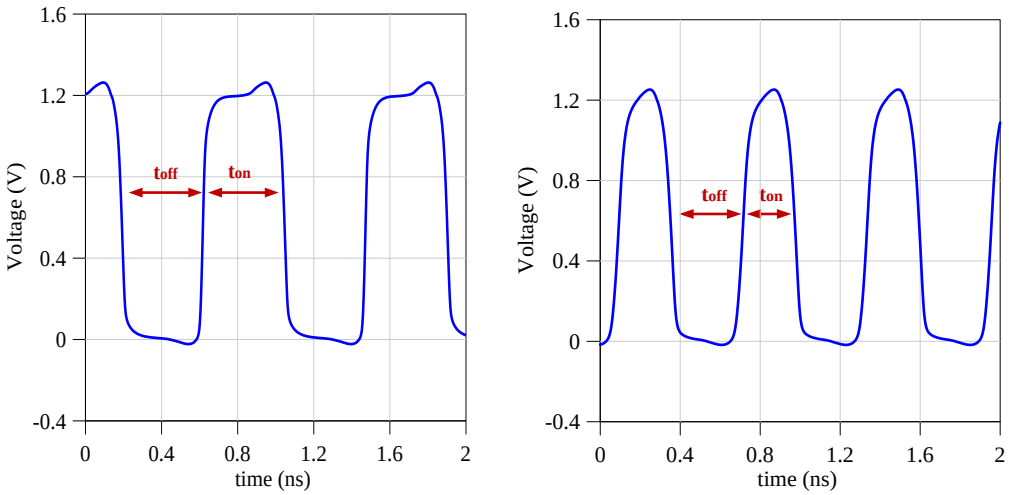

Şekil 11. a) 1200MHz and **b)** 1600MHz signal output.

The duty cycle ratios for 1200MHz and 1600MHz signals are shown in table 4. As shown, the duty cycle for 1200MHz signal is very good, is in acceptable limits for 1600MHz signal output.

Table 4. Duty cycle ratios of signal outputs of the VCO circuit.

Frequency	ton (ps)	toff(ps)	Duty cycle ratio
1200 MHz	391.934	430.924	%47.63
1600 MHz	250.813	369.683	%40.376

3. Results and Disscussion

As seen in Figure 12, the LDO circuit was fed by the current and voltage produced by the temperature-independent bandgap reference circuit. Afterwards, the voltage source required by the VCO circuit was produced with LDO. Thus, all blocks were fed with a single source and the desired square wave production was achieved.

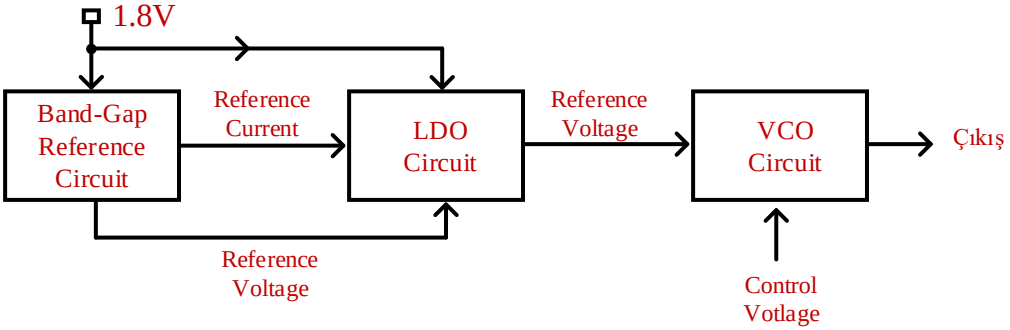

Figure 12. The connection diagram of all presented circuits.

When the band gap reference circuit, LDO circuit and VCO circuit are combined, oscillation is achieved without much performance degradation. All circuits are connected to each other and while the VCO circuit is driving a 0.4pF load, the current provided by the band gap reference

circuit to the LDO circuit is seen in figure 13. Figure 13a shows the current drawn while producing a 1200MHz signal. The pins seen here are a systematic problem caused by the program and do not represent circuit performance. Additionally, as can be seen, the supplied current exhibits a very stable behavior. A similar situation can be seen in figure 13b.

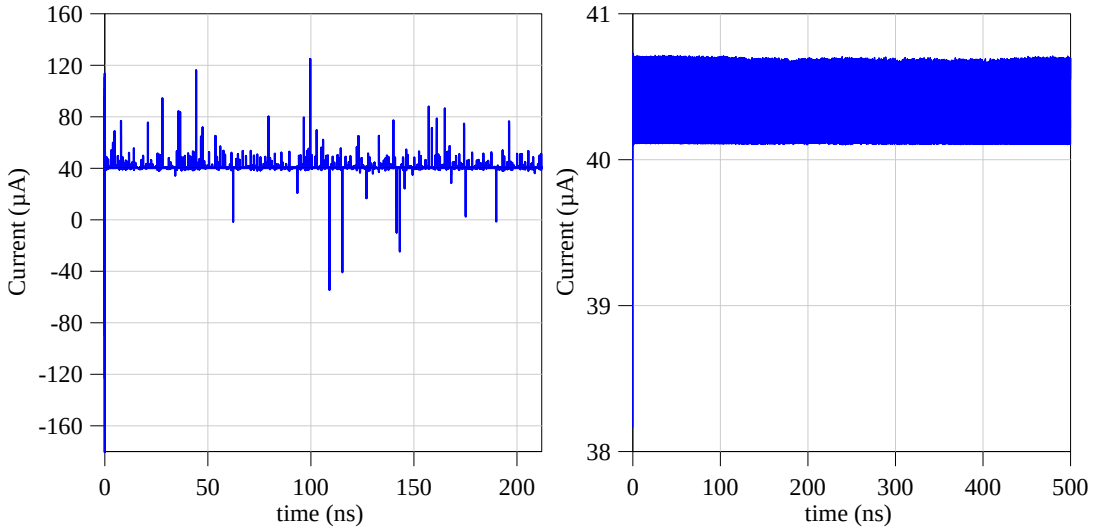

(a) **(b)**

Figure 13. Entire system is interconnected **a)** 1200MHz and **b)** 1580MHz currents provided by the band gap reference circuit for signal outputs.

When all circuits are combined, the outputs of the LDO circuit are seen in the graphs below for 1200MHz and 1580MHz. As can be seen, both LDO outputs give almost the same result. From here it is understood that the LDO circuit is stable.

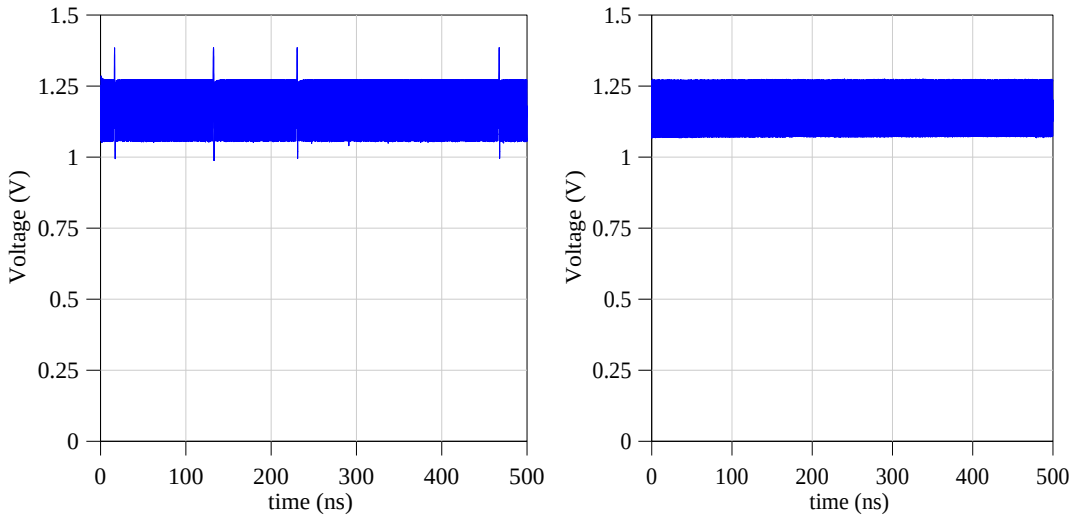

(a) **(b)**

Figure 14. Entire system is interconnected **a)** 1200MHz and **b)** voltage provided by the LDO circuit for 1580MHz signal outputs.

Finally, the VCO output is obtained when all circuits are connected to each other. As seen in Figure 15, it is understood that the square wave shape of the signals produced at both frequencies does not change.

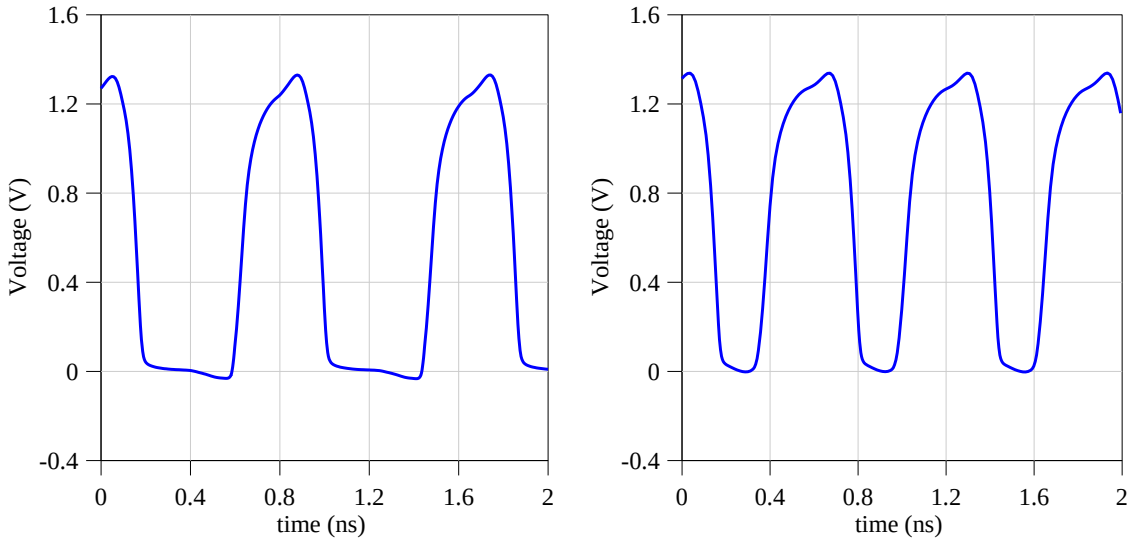

(a) **(b)**

Figure 15. Entire system is interconnected **a)** 1200MHz and **b)** output generated by the VCO circuit for 1580MHz signal outputs.

4. Conclusion

In this study, a bandgap reference voltage circuit was realized by taking advantage of the opposite temperature coefficients of PMOS and NMOS transistors. The circuit exhibited a stable behavior between -40 ºC and 125 ºC and the temperature change was obtained as 5.5 ppm / ºC. The frequency-dependent variation of the PSRR value of the designed circuit between 1 Hz and 10 GHz was found to be -20 dB on average. While the input voltage of the LDO circuit is 1.8V, the output voltage is measured as 1.2V. A square wave between 0V-1.1V was produced with the VCO circuit, and signals at 1.2GHz and 1.6GHz frequencies were obtained with the help of a voltage source. A 0.4pF load was easily driven by the generated square wave. This study shows that the performance of the VCO circuit does not change when examined both under load and no load. Finally, all circuits were connected to each other, the performance of the entire system was examined, and the circuit block fed by a single high-performance source was successfully operated.

Ethics in Publishing

There are no ethical issues regarding the publication of this study.

Author Contributions

Müslüm GÜR: Circuit Designs, Evaluation of the results, Writing – original draft preparation. Yunus BABACAN: Circuit Designs, Evaluation of the results, Supervision, reviewing and editing.

References

[1] Lin, T., Chong, K. S., Chang, J. S., & Gwee, B. H. (2012) An Ultra-Low Power Asynchronous-Logic In-Situ Self-Adaptive $ V_ {\rm DD} $ System for Wireless Sensor Networks. IEEE Journal of Solid-State Circuits, 48 (2), 573-586.

[2] Guo, L., Ge, T., & Chang, J. S. (2014) A 101 dB PSRR, 0.0027% THD+ N and 94% power-efficiency filterless class D amplifier. IEEE Journal of Solid-State Circuits, 49 (11), 2608-2617.

[3] Lee, I., Sylvester, D., & Blaauw, D. (2017) A subthreshold voltage reference with scalable output voltage for low-power IoT systems. IEEE Journal of Solid-State Circuits, 52 (5), 1443-1449.

[4] Wang, Q., Wang, X., Li, J., & Liu, Y. (2022) A bandgap reference voltage source design for wide temperature range. In 2022 7th International Conference on Integrated Circuits and Microsystems (ICICM) (pp. 245-250). IEEE.

[5] Jain, S., Kanchetla, V. K., & Zele, R. (2022) A Sub-1V, current-mode bandgap voltage reference in standard 65 nm CMOS process. In 2022 IEEE 15th Dallas Circuit And System Conference (DCAS) (pp. 1-5). IEEE.

[6] Basyurt, P. B., Bonizzoni, E., Maloberti, F., & Aksin, D. Y. (2017) A low-power low-noise CMOS voltage reference with improved PSR for wearable sensor systems. In 2017 IEEE International Symposium on Circuits and Systems (ISCAS) (pp. 1-4). IEEE.

[7] Shrivastava, A., Craig, K., Roberts, N. E., Wentzloff, D. D., & Calhoun, B. H. (2015) 5.4 A 32nW bandgap reference voltage operational from 0.5 V supply for ultra-low power systems. In 2015 IEEE International Solid-State Circuits Conference-(ISSCC) Digest of Technical Papers (pp. 1-3). IEEE.

[8] Lu, Y., Wang, Y., Pan, Q., Ki, W. H., & Yue, C. P. (2015) A fully-integrated low-dropout regulator with full-spectrum power supply rejection. IEEE Transactions on Circuits and Systems I: Regular Papers, 62 (3), 707-716.

[9] Bu, S., Leung, K. N., Lu, Y., Guo, J., & Zheng, Y. (2018) A fully integrated low-dropout regulator with differentiator-based active zero compensation. IEEE Transactions on Circuits and Systems I: Regular Papers, 65 (10), 3578-3591.

[10] Qu, W., Singh, S., Lee, Y., Son, Y. S., & Cho, G. H. (2016) Design-oriented analysis for Miller compensation and its application to multistage amplifier design. IEEE Journal of Solid-State Circuits, 52 (2), 517-527.

[11] Rajalingam, P., Jayakumar, S., & Routray, S. (2021) Design and analysis of low power and high frequency current starved sleep voltage controlled oscillator for phase locked loop application. Silicon, 13 (8), 2715-2726.

[12] Aranda, M. L., Díaz, O. G., & Álvarez, C. R. B. (2013) A performance comparison of CMOS voltage-controlled ring oscillators for its application to generation and distribution clock networks. Sci J Circuits Syst Sig Process, 2 (2), 56-66.

[13] Hwang, I. C., Kim, C., & Kang, S. M. (2004) A CMOS self-regulating VCO with low supply sensitivity. IEEE Journal of Solid-State Circuits, 39 (1), 42-48.

[14] Jiang, J., Shu, W., & Chang, J. S. (2016) A 5.6 ppm/° C temperature coefficient, 87-dB PSRR, sub-1-V voltage reference in 65-nm CMOS exploiting the zero-temperature-coefficient point. IEEE Journal of Solid-State Circuits, 52 (3), 623-633.

[15] Sobhan Bhuiyan, M. A., Hossain, M. R., Minhad, K. N., Haque, F., Hemel, M. S. K., Md Dawi, O., & Ooi, K. J. (2022) CMOS low-dropout voltage regulator design trends: an overview. Electronics, 11 (2), 193.

[16] Kang, J. G., Park, J., Jeong, M. G., & Yoo, C. (2021) Digital low-dropout regulator with voltage-controlled oscillator based control. IEEE Transactions on Power Electronics, 37(6), 6951-6961.

[17] Kang, J. G., Park, J., Jeong, M. G., & Yoo, C. (2021) Digital low-dropout regulator with voltage-controlled oscillator based control. IEEE Transactions on Power Electronics, 37(6), 6951-6961.

[18] Silva-Martinez, J., Liu, X., & Zhou, D. (2020) Recent advances on linear low-dropout regulators. IEEE Transactions on Circuits and Systems II: Express Briefs, 68(2), 568-573.

[19] Cao, H., Yang, X., Li, W., Ding, Y., & Qu, W. (2021) An impedance adapting compensation scheme for high current NMOS LDO design. IEEE Transactions on Circuits and Systems II: Express Briefs, 68(7), 2287-2291.

[20] Annamma, K., Saxena, S., & Patel, G. S. (2022) Sleepy Stack CSVCO with wide tuning and low power for PLL applications. In Journal of Physics: Conference Series (Vol. 2327, No. 1, p. 012013). IOP Publishing.

[21] Panigrahi, J. K., Acharya, D. P., & Nanda, U. (2022) Performance Analysis of Dual Threshold CMOS based Current Starved Voltage Controlled Oscillator-A Review. In 2022 2nd International Conference on Artificial Intelligence and Signal Processing (AISP) (pp. 1-4). IEEE.

[22] Prajapati, A., & Prajapati, P. P. (2014) Analysis of Current Starved Voltage Controlled Oscillator using 45nm CMOS Technology. International Journal of Advanced Research in Electrical, Electronics and Instrumentation Engineering, 3(3), 8076.